Photoelectron branching ratios and angular distributions for the valence levels of SF₆ in the range $16 \leq hv \leq 30$ eV

J. L. Dehmer

Argonne National Laboratory, Argonne, Illinois 60439

A. C. Parr

Synchrotron Ultraviolet Radiation Facility, National Bureau of Standards, Washington, D.C. 20234

Scott Wallace

Department of Materials Science and Engineering, Massachusetts Institute of Technology, Cambridge, Massachusetts 02139

Dan Dill

Department of Chemistry, Boston University, Boston, Massachusetts 02215

Photoelectron branching ratios and angular distributions have been measured for the six outermost levels of SF_6 in the range $16 \leq hv \leq 30$ eV with the use of synchrotron radiation. These results are discussed in the framework of the large variety of experimental and theoretical studies of SF_6 with the dual objective of resolving the long-standing problem of the ordering of the valence shells and of gaining some insight into the role of shape-resonant behavior in the low-energy photoionization continua of SF_6. These objectives are met with partial success in that we tentatively conclude the valence configuration $5a_{1g}^2 4t_{1u}^6 1t_{2g}^6 3e_g^4 (1t_{2u}^6 + 5t_{1u}^6) 1t_{1g}^6 \, {}^1A_{1g}$ is most consistent with the available body of evidence and that it is plausible to invoke channel interaction near the strong resonant feature at $hv \sim 23-24$ eV to help account for some of the apparently contradictory evidence. Further experimental and theoretical work is suggested to clarify these issues.

I. INTRODUCTION

The photoionization of SF_6 has been avidly studied over the past 10–15 years. One inducement has been its octahedral symmetry, which should render the study of its spectral properties more tractable than for other large polyatomics. Another, less trivial, motivation has been the central role played by SF_6 in the elucidation of shape-resonance effects in molecules. The four shape-resonant features (a_{1g}, t_{1u}, t_{2g}, and e_g) in the sulfur K-shell[1] and L-shell[2] spectra remain the most striking examples of potential barrier effects in molecular spectra.[3]

For these and other reasons, a large amount of information has been generated on SF_6 photoionization and related excitation processes: On the theoretical side, several groups have calculated the electronic structure[4-8] of SF_6, and others have calculated partial photoionization cross sections[9-13] and photoelectron angular distributions[12,13] for all the subshells of SF_6. In addition, the elastic e-SF_6 scattering cross section[14,15] has been calculated indi-

cating the role of the above-mentioned shape resonances and the close connection[16] between shape resonances in electron scattering and photoionization contexts. An even larger collection of experimental work includes (i) x-ray absorption and emission cross sections from core levels,[1,2,17-20] (ii) vuv absorption by valence levels,[19,21-24] (iii) photoelectron spectra using x-rays[25] and vuv resonance lines,[25-28] (iv) photoelectron angular distributions with HeI radiation,[27] (v) partial photoionization cross sections using synchrotron radiation,[28] (vi) photoionization mass spectrometry and ionization yield measurements,[29,30] and (vii) electron scattering measurements of total scattering,[31] differential elastic scattering,[32] and inelastic scattering in the low-energy,[33,34] pseudo-optical limit,[35] and $(e,2e)$[36] configurations.

Despite this great body of information, however, there remain major unsolved questions concerning the spectroscopy and dynamics of SF_6 photoionization. The two issues of concern here are the ordering of the valence levels of SF_6 and the role of the t_{2g} shape resonance in valence-shell spectra. Con-

cerning the ordering of valence levels, several ground-state configurations have been proposed on the basis of different types of evidence, but, as of yet, there is no broad consensus. This issue is complicated by the near degeneracy of two valence levels (which two is one of the central questions), resulting in the occurrence of six photoelectron peaks in the binding energy (BE) range $16 \text{ eV} \leq \text{BE} \leq 30$ eV, where seven valence levels are known to lie. The study of shape resonance effects in valence-shell spectra depends very much on establishing the ground-state configurations as, *in the independent electron approximation,* dipole selection rules govern which orbitals will make transitions to particular shape resonances. The significance of the qualification in italics will be discussed later.

In this paper, we present new evidence and review the existing literature in an attempt to resolve these problems. In particular, we present new measurements of partial photoionization cross sections, branching ratios, and photoelectron angular distributions for the valence levels of SF_6 in the photon range $16 \text{ eV} \leq h\nu \leq 30$ eV. The partial cross sections and branching ratios agree well with those measured earlier by Gustafsson[28] where the two sets of data overlap. In addition, we present multiple-scattering calculations[12] of the same quantities. The theoretical calculations will be described in detail elsewhere.[13] They are used here in a form chosen specifically for extracting the needed information from the data. Namely, they have been convoluted with the experimentally observed peak shapes and are plotted in alternative ways to illustrate the consequences of adopting various valence-level orderings. In the discussion of the results, we conclude that the most plausible valence configuration is

$$5a_{1g}^2 4t_{1u}^6 1t_{2g}^6 3e_g^4 (1t_{2u}^6 + 5t_{1u}^6) 1t_{1g}^6 \, {}^1A_{1g} \, ,$$

although some small uncertainty still exists regarding the location of the $1t_{2u}$ level. We conclude by proposing further experimental and theoretical work to test our conclusions and to study the strong channel interaction effects implied by them.

II. EXPERIMENT

The apparatus used in this work has been described in detail elsewhere[37] and will only be discussed briefly here. The variable wavelength light was obtained from a high-aperture 2-meter, normal-incidence monochromator[38] attached to the National Bureau of Standards (SURF-II) storage ring. With a 1200-line/mm grating, a virtual entrance slit (the stored electron orbit), and a 100-μm exit slit, this instrument produced a spectral resolution of 0.4-Å full width at half maximum (FWHM) and flux of 5×10^{10} photons $\sec^{-1} \text{Å}^{-1}$ at 600 Å with a typical 10-mA beam circulating in the storage ring. The ejected electrons were energy analyzed by a 2-in. mean-radius hemispherical analyzer operated at a constant resolution of 110 meV. The analyzer was calibrated with the use of Ar gas whose photoionization cross section[39] and photoelectron asymmetry parameters[40−42] are known in this wavelength range. As the light from the monochromator was elliptically polarized, the differential cross section in the dipole approximation, assuming randomly oriented target molecules, can be written[37,43]

$$\frac{d\sigma}{d\Omega} = (\sigma_{\text{tot}}/4\pi)[1 + \tfrac{1}{4}\beta(3P \cos2\theta + 1)] , \quad (1)$$

where β is the photoelectron asymmetry parameter, θ is the photoelectron ejection angle relative to the major polarization axis, and

$$P = (I_{||} - I_{\perp})/(I_{||} + I_{\perp})$$

is the polarization of the light which was measured with a three-mirror polarization analyzer.[37]

At each wavelength reported here, photoelectron spectra of all energetically accessible valence states of SF_6 were recorded at $\theta = 0°$, 45°, and 90°. At each angle the net counts in each photoelectron peak were summed, and the integrated counts were corrected for the transmission function of the electron spectrometer and a small $<4\%$ angular correction factor based on the aforementioned electron spectrometer angular calibration. The asymmetry parameter β was then determined for each peak by means of Eq. (1), and photoionization branching ratios were determined by comparing the relative peak intensities at the magic angle $\theta = 58°$, as deduced from Eq. (1), with the use of the intensities at the measured angles and the measured β values. Partial photoionization cross sections were then determined for each state by taking the product of the branching ratio and the absolute, total ionization cross section reported by Hitchcock *et al.*[35] The errors quoted in the next section represent a combination of the statistical uncertainty of the integrated peak intensities and the degree of agreement between the parameters deduced from the redundant set of measurements at three angles.

III. RESULTS

There are seven occupied valence states of SF_6 with ionization potentials (IP's) less than 30 eV,[25-38] all derived from the fluorine $2p$ and sulfur $3s$, $3p$, and $3d$ atomic orbitals. Their approximate ordering starting with the least tightly bound is $1t_{1g}^6$, $5t_{1u}^6$, $1t_{2u}^6$, $3e_g^4$, $1t_{2g}^6$, $4t_{1u}^6$, and $5a_{1g}^2$ combining to give a closed-shell ground state with $^1A_{1g}$ symmetry. The photoelectron spectrum[25-28] covering this range of IP's exhibits six peaks with vertical IP's of 15.7, 17.0, 18.6, 19.7, 22.5, and 26.8 eV. In the following, we will refer to these as peak 1 through peak 6, respectively, in order of increasing IP. Clearly, one of the peaks encompasses two IP's, and the probable candidates are peak 2 and peak 3. This will be the main focus of the next section. Peak 6 is easily and unanimously assigned to the $5a_{1g}$ molecular orbital (MO) and is not discussed further here since its branching ratio is always $< 2\%$ for $hv < 30$ eV,[28] and it was not well characterized in the measurements presented here.

Our experimental results are presented in Figs. 1−5 for peaks 1−5, respectively, along with corresponding theoretical results which will be described below. In each figure, the top frame contains the photoelectron asymmetry parameter β from the IP up to $hv = 29.2$ eV. The β values tend to gravitate around $\beta = 0$, and the resulting nearly isotropic distribution was easily measured with good precision. The average uncertainty was ± 0.03 with the largest being ± 0.1. Including the uncertainty in the calibration procedure, we assign an overall accuracy of approximately ± 0.05 to the β values. Differences of up to 0.15 were noted relative to earlier measurements[27] of β at 584 Å; however, for all but peak 1, our β's lay in the range of β's measured across the bands in Ref. 27. Some discussion of the variation of β's across peaks 2 and 3 is given at the end of this section. In view of the likelihood of autoionization near 22.2 eV,[21] we are not greatly concerned with the differences observed using our medium-resolution light source and the narrow-band resonance line.

The second frame in Figs. 1−5 gives the branching ratios of peaks 1−5 relative to the sum of their intensities. Uncertainties in these quantities are typically ± 0.01. Agreement with earlier measurements by Gustafsson[28] is generally good, although local differences of 0.05 are observed. Differences in energy mesh, transmission function calibrations for low kinetic energies, and the β dependence of the earlier measurements[28] probably contribute to this, although the differences do not significantly
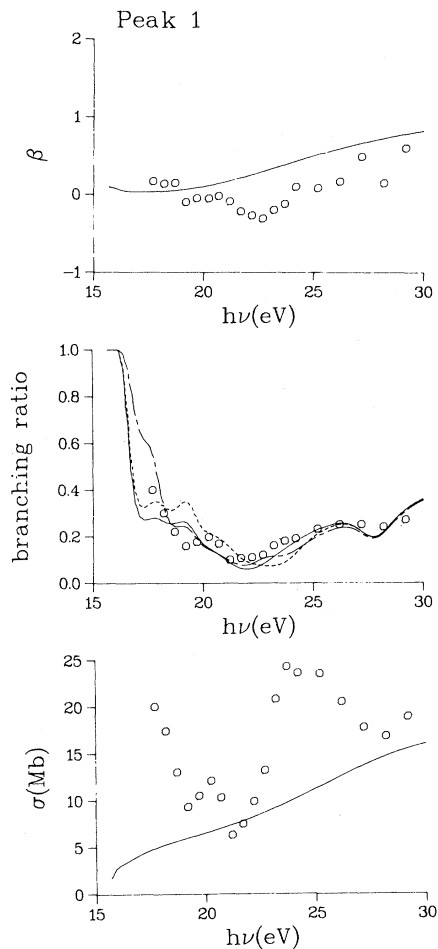

FIG. 1. Photoelectron asymmetry parameter, branching ratio, and partial cross section for peak 1 (IP = 15.7 eV). Open circles are present data. Curves are theoretical calculations as described in Sec. III.

affect the following discussion.

The lower frame in Figs. 1−5 contains the partial cross section for peaks 1−5, obtained by multiplying the measured branching ratios times the total ionization cross section (total photoabsorption cross section multiplied by the ionization efficiency) reported by Hitchcock et al.[35] Again semiquantitative agreement was observed with the analogous analysis by Gustafsson,[28] who used total absorption data by Lee et al.[23] The total absorption cross sections by Hitchcock et al.[35] and Lee et al.[23] are in good agreement throughout the range discussed here. The only significant issue is the assumption by Gustafsson[28] that the ionization efficiency is unity throughout this range. The ionization efficiency measured by Hitchcock et al.[35] was greater than 90% for $hv > 20$ eV, but fell off toward the ionization threshold to a value of 25% at $hv = 16$ eV.
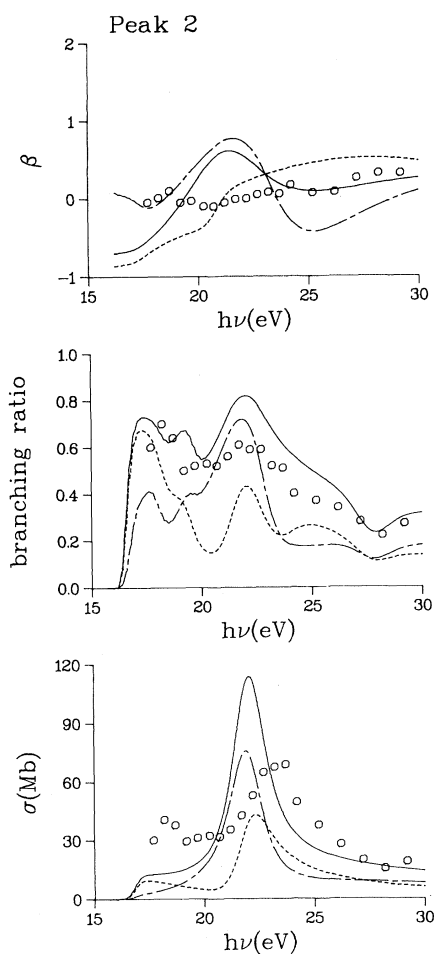
FIG. 2. Photoelectron asymmetry parameter, branching ratio, and partial cross section for peak 2 (IP = 17.0 eV). Open circles are present data. Curves are theoretical calculations as described in Sec. III.
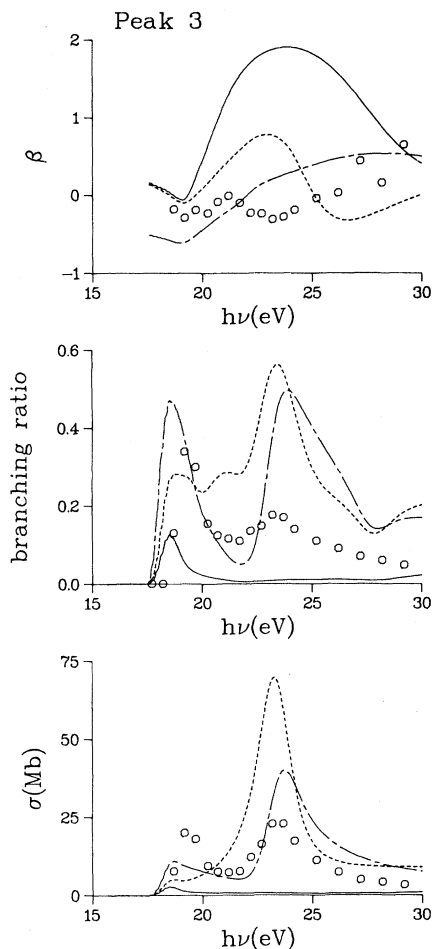

FIG. 3. Photoelectron asymmetry parameter, branching ratio, and partial cross section for peak 3 (IP = 18.6 eV). Open circles are present data. Curves are theoretical calculations as described in Sec. III.

This accounts for some, but by no means all, of the quantitative differences between the data sets. The observed semiquantitative agreement is considered satisfactory for this type of measurement at this time, and, although it would be desirable to remove the remaining minor discrepancies, they pose no significant problem vis-á-vis the issues discussed in the next section. There, the occurrence of peaks in the partial cross sections represents the most significant aspects of the data; and, on this point, there is no qualitative disagreement.

The continuous curves in Figs. 1 — 5 are theoretical results for each measured quantity. They have been presented in the following manner to try to aid in resolving assignments in valence shell photoionization of SF_6 by use of dynamical evidence. *First*, the partial cross section and photoelectron asymmetry parameter for each valence state of SF_6 was

calculated[12,13] using the multiple-scattering model by now standard procedures.[44] These calculations will be presented and discussed in detail elsewhere.[13] *Second*, three sets of theoretical curves were derived as described in Table I, each set corresponding to one of the possible valence configurations discussed later, each differing in the assignment of the $5t_{1u}$, $1t_{2u}$, and $3e_g$ initial states to peaks 2 and 3. *Third*, each set of dipole matrix elements and asymmetry parameters was combined with the corresponding experimental IP's, consistent with the assignments in that set, and was then folded with Gaussian line shapes with the half widths in the experimental spectrum (0.4, 0.6, 0.7, 0.7, and 0.4 eV for peaks 1 — 5, respectively). This avoided sudden jumps in the branching ratios at higher IP's and ensured the comparison between experiment and theory was not confused by the intrinsic and instrumental widths
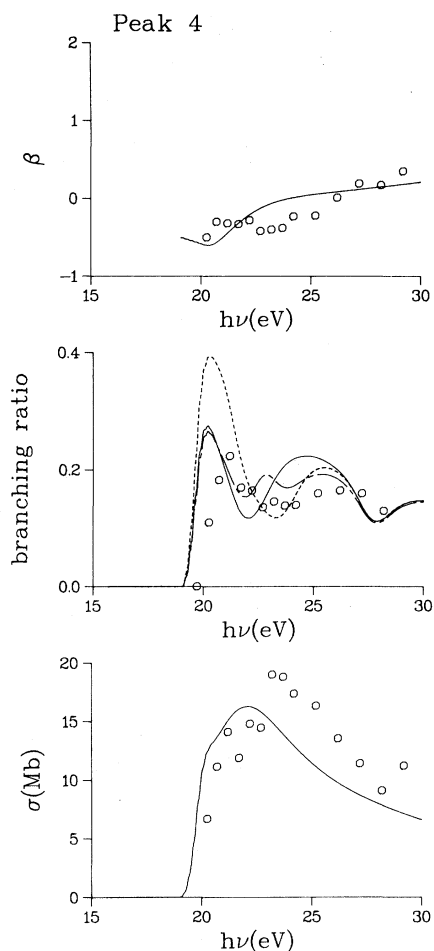
FIG. 4. Photoelectron asymmetry parameter, branching ratio, and partial cross section for peak 4 (IP = 19.7 eV). Open circles are present data. Curves are theoretical calculations as described in Sec. III.

FIG. 5. Photoelectron asymmetry parameter, branching ratio, and partial cross section for peak 5 (IP = 22.5 eV). Open circles are present data. Curves are theoretical calculations as described in Sec. III.

of the photoelectron peaks.

In Fig. 6, we show some typical data at $hv = 20.25$ eV where the doubling in peak 3 is apparent. This has been observed by previous authors.[25−28] In Fig. 7, however, we show that at $hv = 22.2$ eV, pronounced doubling also occurs in

peak 2, at which wavelength peak 3 does not exhibit clear doubling. This doubling can be due to Jahn-Teller splitting, the effects of two overlapping bands, or final state resonance effects such as autoionization. A shoulder on peak 2 was also observed at 584 Å by Sell and Kuppermann[27] and by Gelius,[25] although not as pronounced as in Fig. 7. The point is, *both* controversial peaks, each argued to consist of overlapping bands by various authors, exhibit pronounced doubling at selected wavelengths and angles. Therefore this type of qualitative argument cannot be used to resolve the existing controversy in any straightforward manner.

TABLE I. Trial assignments used to construct theoretical curves in Figs. 1 — 5.

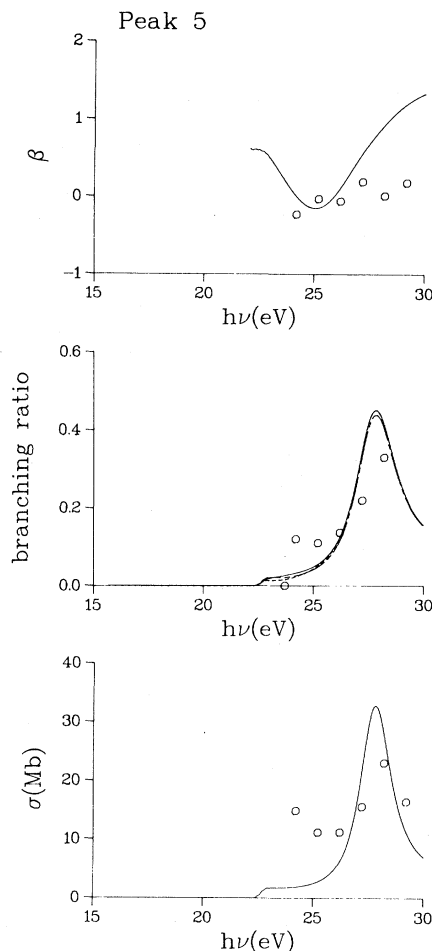| Peak number	Solid curve	Dashed curve	Dash-dot curve
1	$1t_{1g}$	$1t_{1g}$	$1t_{1g}$
2	$1t_{2u} + 5t_{1u}$	$5t_{1u}$	$1t_{2u}$
3	$3e_g$	$1t_{2u} + 3e_g$	$5t_{1u} + 3e_g$
4	$1t_{2g}$	$1t_{2g}$	$1t_{2g}$
5	$4t_{1u}$	$4t_{1u}$	$4t_{1u}$

IV. DISCUSSION

To simplify the discussion of the complex body of data bearing on this subject, we will proceed by

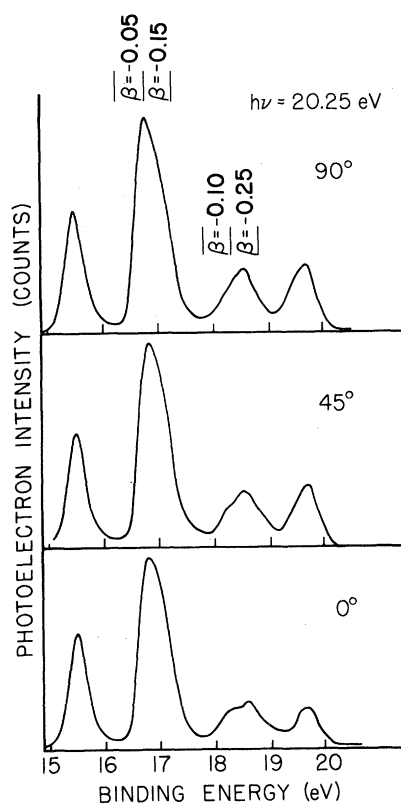FIG. 6. Photoelectron spectra of SF_6 at $h\nu=20.25$ eV and $\theta=0°$, 45°, and 90°.

FIG. 7. Peaks 2 and 3 of the photoelectron spectra of SF_6 at $h\nu=22.2$ eV and $\theta=0°$, 45°, and 90°, showing the doubling in peak 2.

presenting a recommended valence-level structure, followed first by evidence supporting this conclusion and second by a discussion of various aspects of the assignment, including a tentative rationalization of seemingly contradictory evidence. Accordingly, we will consider the assignment of photoelectron peaks 1—5 to ionization from $1t_{1g}$, $5t_{1u}+1t_{2u}$, $3e_g$, $1t_{2g}$, and $4t_{1u}$ MO's, respectively. This is also the ordering arrived at in earlier theoretical work by Connolly and Johnson,[5] Hay,[7] and von Niessen et al.,[6,8] and in experimental work by Gelius.[25]

General support for the above ordering is provided by the results of the two most sophisticated calculations of SF_6 electronic structure, namely, the many-body Green's-function calculations of von Niessen et al.[6,8] and the generalized valence-bond calculations of Hay.[7] Both types of calculations yield the above sequence of MO's, and the ordering predicted by the calculations by von Niessen et al. was found[8] to be extremely stable with respect to large changes of basis functions and other conditions. In fact, in all calculations we are aware of only the relative ordering of the $5t_{1u}$ and the $1t_{2u}$,
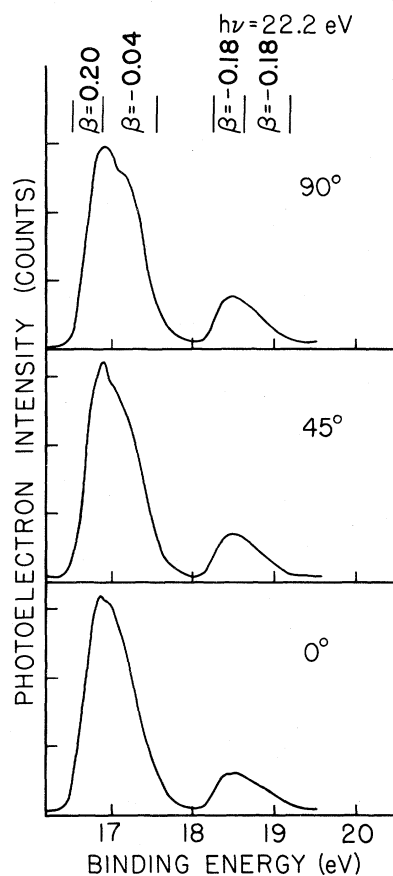
and the question of their quasidegeneracy varies.

Important experimental evidence is provided by x-ray emission resulting from filling holes in the sulfur $1s$ and $2p$ subshells by dipole transitions from the valence shells. Sulfur K x-ray emission spectra reported by LaVilla[18] locate the $3t_{1u}$, $4t_{1u}$, and $5t_{1u}$ valence levels and provide concrete confirmation of the $4t_{1u}$ and $5t_{1u}$ assignments given above. More recent, high-resolution x-ray emission spectra[20] for the sulfur L shell likewise locate the $5a_{1g}$, $1t_{2g}$, and $3e_g$ levels and provide concrete confirmation of the $3e_g$ and $1t_{2g}$ assignments given above. To summarize the x-ray emission evidence, the $5t_{1u}$, $3e_g$, $1t_{2g}$, and $4t_{1u}$ levels are associated with peaks 2, 3, 4, and 5, respectively.

This leaves the placement of the $1t_{1g}$ and $1t_{2u}$ orbitals. We conform to the assignment of the $1t_{1g}$ orbital to peak 1. There is little qualitative evidence for this (the t_{1g} does not have a dipole allowed component on the sulfur atom which would be active in the sulfur L emission spectrum); however, there is nearly universal agreement on this assignment. The

placement of the $1t_{2u}$, on the other hand, is the most controversial assignment. We assign it to peak 2 mainly on the evidence of the x-ray photoelectron spectrum, as interpreted by Gelius.[25] At $h\nu = 1.25$ keV, the second peak in the photoelectron spectrum is approximately twice as large as the first, third, or fourth. As all of these are derived mainly from fluorine p orbitals, this suggests that the second peak consists of two overlapping bands. This is a simplified version of Gelius' more detailed analysis in terms of net atomic populations. Note also that in all recorded photoelectron spectra at any wavelength, peak 2 is significantly larger than peak 3. This concludes the main arguments supporting the recommended assignment. Note that it relies heavily on x-ray data, which, as we shall suggest later, is valuable in that it should be free from gross channel interaction effects that are believed to significantly modify valence shell dynamics. Note also that this conclusion means that the doubling in peak 2 probably arises from the superposition of two peaks (although other causes could also distort the photoelectron peak) and that peak 3 is split at certain wavelengths and angles by the Jahn-Teller effect.

The major difficulty with the above picture arises from work by Gustafsson,[28] who used partial cross section measurements, and earlier evidence[3] that a shape resonance occurs at ~ 5-eV kinetic energy in the t_{2g} continuum, to conclude that peaks 2 and 3 corresponded to ionization from the $5t_{1u} + 3e_g$ and $1t_{2u}$ MO's, respectively, with the possible interchange of the two odd-parity MO's. This was later discussed in connection with multiple-scattering calculations with the same general conclusions,[11] although the $5t_{1u}$ and $1t_{2u}$ were switched in that work. The reasoning was the following. Since a final-state shape resonance of t_{2g} symmetry is known to lie at ~ 5-eV kinetic energy, photoelectron peaks which are significantly enhanced approximately 5 eV above their respective IP's will be odd levels which couple to the t_{2g} resonance in a dipole transition. Peaks 2, 3, and 5 were observed to resonate between 5 and 6 eV above threshold, and therefore they would be assigned to the odd levels $5t_{1u}$, $1t_{2u}$, and $4t_{1u}$ with some ambiguity concerning the first two. Gustafsson used the x-ray photoelectron intensity arguments employed above to conclude peak 2 contained two peaks and therefore the $3e_g$. It is now fairly clear from x-ray emission data that the $5t_{1u}$ and $3e_g$ levels are associated with peaks 2 and 3, respectively. However, the argument that peak 3 resonates at 5-eV kinetic energy, and therefore contains the $1t_{2u}$ peak is a serious con-

tradiction to the assignment proposed earlier, particularly since our data confirm the resonant behavior and the existence of the t_{2g} shape resonance is well established.

We tentatively resolve this dilemma by attributing the resonant activity of peak 3 to some form of channel interaction whereby peak 3 shares in the huge resonant enhancement of peak 2 at $h\nu \sim 23 - 24$ eV. The coupling could be direct Coulomb coupling between the nearly degenerate channels since the excited complex (ion plus photoelectron) has the same symmetry, or possibly vibronic coupling. The latter may be enhanced (relative to typical direct molecular photoionization) since the electron is resonantly trapped, and hence delayed in its escape, and the SF_6^+ ion is known to be unstable relative to fragments of lower symmetry. This conjecture is nebulous and would require more theoretical study to demonstrate its validity. However, it is supported by the following observations. *First*, strong channel interaction resulting in intensity borrowing in the vicinity of the strong resonant enhancement at $h\nu \sim 23$ eV in the total cross section would tend to occur near this photon energy. Indeed, peaks 2 and 3 reach a maximum at $h\nu \sim 23$ eV and are better aligned than on a kinetic energy scale. *Second*, peak 1, almost surely involving an even initial state, also peaks at $h\nu \sim 23$ eV when the sloping background is taken into account (see Fig. 1). In fact, the local enhancement at $h\nu \sim 23$ eV in peak 1 is the same magnitude (~ 15 Mb) as that in peak 3. The enhancement is more clearly displayed in Fig. 1 than in Gustafsson's data,[28] but both exhibit a clear rise at $h\nu \sim 22 - 23$ eV, which is totally absent from the one electron calculations. *Third*, the appearance of symmetry-forbidden transitions to shape resonant features has already been noted[3] in inner-shell absorption spectra for SF_6, e.g., the t_{1u} shape resonance is seen as a weak bump in the sulfur $2p$ absorption spectra, and the a_{1g}, t_{2g}, and e_g resonant feaures align with weak features in the sulfur $1s$ spectra, when the spectra's IP's are aligned. The coupling in the x-ray spectra is weak, only a few present, whereas one would have to postulate coupling on the order of 20% in the valence shell; but the qualitative trend is reasonable owing to the quasidegeneracy in the valence spectra.

Another possible source for deviations from the independent-electron reasoning regarding the appearance of resonant enhancements in the partial cross sections is autoionization structure, particularly that involving the shape resonantly enhanced antibonding $6a_{1g}$ and $6t_{1u}$ MO's, known to cause strong features[3] below inner-shell thresholds. If one

of these states occurred near $hv \sim 23$ eV, this could perturb the simplified shape-resonance picture. The two most likely candidates are the $5a_{1g} \rightarrow 6t_{1u}$ and the $4t_{1u} \rightarrow 6a_{1g}$ transitions. Taking the kinetic energy of the $2t_{2g}$ shape resonance as ~ 5.7 eV and the $6a_{1g}$-t_{2g} and $6t_{1u}$-t_{2g} spacings from x-ray absorption data, we arrive at transition energies of $hv \sim 17.2$ eV and 26.7 eV for the $5a_{1g} \rightarrow 6t_{1u}$ and the $4t_{1u} \rightarrow 6a_{1g}$ transitions, respectively. (Note that shape-resonant features shift by $\sim 1 - 3.5$ eV toward higher kinetic energy in going from inner-shell to valence-shell spectra due to different screening and other differences in relaxation effects; therefore, we approximate relative energies from x-ray spectra, but normalize to the t_{2g} in the valence-shell spectra.) Neither matches the position of the main resonance peak at $hv \sim 23$ eV; however, we note in passing that the total ionization cross section has an unidentified peak at $hv \sim 17$ eV. Hence the $6a_{1g}$ and $6t_{1u}$ excited states do not appear to bear on the present discussion. Other weaker, nonresonantly enhanced autoionization states are known to be in this region[21] and may cause departures from a one-electron framework of interpretation. However, the observed structures are weak relative to the magnitude of the resonant enhancements in peaks 1 and 3; and therefore, we tentatively discount the importance of autoionizing Rydberg states in this connection.

Against this background, we now examine the experimental and theoretical results presented in Figs. 1—5. In assessing the agreement between experiment and theory, recall that in most diatomic and triatomic cases studied, the independent-electron multiple-scattering model achieves qualitiative to semiquantitative agreement with shape-resonant and nonresonant photoionization.[12] The β's are usually within 0.25 of a β unit and have the same general shape as the data. The partial cross sections exhibit all known shape resonances, although the theoretical resonance line shape tends to be too intense and narrow relative to the data and may be shifted by $1-2$ eV. Nuclear motion and electron correlation tend to smear out these sharp features. We might expect good agreement for SF_6 owing to the favorable close-packed geometry, which should minimize the impact of assumptions inherent in the multiple-scattering potential. However, anticipating our results, we find qualitative departures in the vicinity of the major resonance at $hv \sim 23$ eV and better agreement away from this main resonant peak, which tends to support the idea that the one-electron channels are exhibiting strong channel interaction enhanced near the t_{2g} shape resonance.

In Fig. 1, the β computed for the $1t_{2g}$ MO agrees satisfactorily with the data. The measured branching ratio also agrees well with the calculations, regardless of how the assignments for peaks 2 and 3 are chosen. The base level of the partial cross section also agrees well with the calculated curve, although significant enhancements exist at threshold and at $hv = 23 - 24$ eV, i.e., where large peaks occur in the total cross section, as noted above. We therefore conclude, in the context of the above discussion, that the dynamical information is consistent with the assignment of peak 1 to ionization of the $1t_{1g}$ valence orbital with significant coupling near strong resonances in other channels. Note that the branching ratio and partial cross section give rather different overall impressions about the agreement between experiment and theory. This arises since a small difference in the branching ratio can be amplified in the partial cross section by a large peak in the total ionization cross section. Moreover, differences in wavelength scale and bandwidth between the total-ionization and photoelectron measurements can produce artificial structure, although that is not believed to be a problem with the broad structures involved here.

In Fig. 2, the comparisons with different assignments do not immediately suggest that the recommended solid curve ($5t_{1u} + 1t_{2u}$ in peak 2) agrees better with the data. However, the following points offer some support. First, beyond the resonance peak, $hv > 26$ eV, the data fall closest to the solid line. Second, this is also true at higher energies, e.g., $hv \sim 50$ eV, where peaks 2 and 3 have cross sections of ~ 16 Mb and ~ 6 Mb, respectively,[28] which is reasonably in agreement with the solid line which goes to 13 and 5.5 Mb for peaks 2 and 3, respectively.[11-13] Third, only the solid curve exceeds the experimental peak which, as stated above, is most often found in such comparisons. It should be mentioned that the $1t_{2u}$ is responsible for $\sim \frac{2}{3}$ of the cross section in the peak, as indicated by the dash-dot curve so that its presence in the most intense channel (peak 2) is strongly suggested. Note also that the excess of theoretical cross section over experimental cross section roughly equals the magnitude of the resonant enhancement in peaks 1 and 3 at $hv \sim 23$ eV.

In Fig. 3, the calculations all badly fail to account for major aspects of the data. The β, branching ratio, and partial cross section data depart qualitatively from the solid curves, particularly near $hv \sim 23$ eV. At the highest energy they begin to converge, and at $hv \sim 50$ eV the $3e_g$ cross section is ~ 6 Mb,[28] in good agreement with the calculated

value of 5.5 Mb.[11-13] We therefore ascribe the enhanced cross section of peak 3 at $hv \sim 23$ eV to intensity borrowing from the intense nearly degenerate channel represented by peak 2. This assignment is made difficult by the fairly good agreement between the dash-dot curve and the cross section data and the β data in Fig. 3; however, adoption of the dash-dot convention is in direct opposition to LaVilla's convincing argument based on x-ray emission data.[18] Obviously, this is the main conflict to be resolved in future work.

In Fig. 4, the overall agreement with the solid curve is very good, lending dynamical support to the assignment of peak 4 to ionization of the $1t_{2g}$ MO. In Fig. 5, the appearance of the resonant enhancement at ~ 5.5-eV kinetic energy indicates the action of the t_{2g} shape resonance in this channel and supports its assignment to $4t_{1u}$ ionization as suggested by Gustafsson[28] and others.

V. CONCLUSION

To summarize, we have examined diverse evidence, including the present work, concerning valence shell photoionization of SF_6. We have tentatively concluded that the valence configuration

$$\cdot \; 5a_{1g}^2 4t_{1u}^6 1t_{2g}^6 3e_g^4 (1t_{2u}^6 + 5t_{1u}^6) 1t_{1g}^6 \; {}^1A_{1g}$$

is most consistent with the most definitive evidence. We note that apparent contradictions, such as the comparison of the data and the solid curve in Fig. 3, are serious challenges to our conclusions. However, these contradictions are based on an independent-electron picture of valence shell photoionization in SF_6. For reasons stated above, we have chosen to postulate strong channel interaction in the vicinity of the very intense t_{2g} shape resonance in the $5t_{1u} + 1t_{2u}$ channel (peak 2) at $hv \sim 23$ eV. If we are correct, this reconfirms that shape-resonant features can be most easily identified in inner-shell spectra, whereas their role in valence-shell spectra can be significantly affected not only by the increased energy dependence of the dipole matrix element, but also by the possibility of strong channel interaction between the more closely spaced optical channels. We wish to state emphatically

that this paper should not be taken as conclusive on these issues. Clearly, more work tailored to this problem area needs to be carried out: Experimentally, it would be beneficial to extend triply differential measurements such as those reported here into the soft x-ray range, say up to $hv \sim 150$ eV, in order to avoid the strong channel interactions at lower energy. Gustafsson reported[28] partial cross sections up to $hv \sim 50$ eV, which do, in fact, tend to support most of our conclusions, although they also raise additional interesting questions concerning the failure to clearly observe the strong e_g shape resonance at ~ 15-eV kinetic energy. Similar arguments to those used here may apply to this problem as well. In addition, high-energy, narrow shape resonances have been found[45] to be significantly smeared out by nuclear motion, which would be especially important for this resonance in SF_6. All these interesting aspects notwithstanding, it would be very useful to move into a region where such effects were absent in order to establish important underlying assignments. On the theory side, it is imperative to begin examining channel interaction and vibrational effects in this and similar systems. Owing to the complexity of SF_6, this is probably only feasible at this time in connection with extensions of the multiple scattering model,[44] used here for independent-electron, fixed nuclei results. We hope that this work will help stimulate some of this much needed advancement of present capabilities, since issues such as those raised here will surely be frequently encountered in the growing body of work in valence-shell photoionization of polyatomics using synchrotron radiation.

ACKNOWLEDGMENTS

[1] R. E. LaVilla and R. D. Deslattes, J. Chem. Phys. 44, 4399 (1966).

[2] T. M. Zimkina and V. A. Fomichev, Dok. Akad. Nauk. USSR 169, 1304 (1966) [Sov. Phys.—Dokl. 11, 726 (1967)].

[3] J. L. Dehmer, J. Chem. Phys. 56, 4496 (1972).

[4] F. A. Gianturco, C. Guidotti, U. Lamanna, and R. Moccia, Chem. Phys. Lett. 10, 269 (1971).

[5] J. W. D. Connolly and K. H. Johnson, Chem. Phys. Lett. 10, 616 (1971).

[6]W. von Niessen, L. S. Cederbaum, G. H. F. Diercksen, and G. Hohlneicher, Chem. Phys. 11, 399 (1975).

[7]P. J. Hay, J. Am. Chem. Soc. 99, 1003 (1977).

[8]W. von Niessen, P. Kraemer, and G. H. F. Diercksen, Chem. Phys. Lett. 63, 65 (1979).

[9]F. A. Gianturco, C. Guidotti, and U. Lamanna, J. Chem. Phys. 57, 840 (1972).

[10]V. P. Sachenko, E. V. Polozhenstev, A. P. Kovtun, Yu. F. Migal, R. V. Vedrinski, and V. V. Kolesnikov, Phys. Lett. 48A, 169 (1974).

[11]H. J. Levinson, T. Gustafsson, and P. Soven, Phys. Rev. A 19, 1089 (1979).

[12]S. Wallace, Ph.D. thesis, Boston University, 1980 (unpublished).

[13]S. Wallace, D. Dill, and J. L. Dehmer (unpublished).

[14]J. L. Dehmer, J. Siegel, and D. Dill, J. Chem. Phys. 69, 5205 (1978).

[15]M. G. Benedict and I. Gyemant, Int. J. Quantum Chem. 13, 597 (1978).

[16]J. L. Dehmer and D. Dill, in *Symposium on Electron-Molecule Collisions,* edited by I. Shimamura and M. Matsuzawa (University of Tokyo Press, Tokyo, 1979), p. 95.

[17]T. M. Zimkina and A. C. Vinogradov, J. Phys. (Paris) Colloq. 32, 3 (1971).

[18]R. E. LaVilla, J. Chem. Phys. 57, 899 (1972).

[19]D. Blechschmidt, R. Haensel, E. E. Koch, U. Nielsen, and T. Sagawa, Chem. Phys. Lett. 14, 33 (1972).

[20]H. Ågren, J. Nordgren, L. Selander, C. Nordling, and K. Siegbahn, Phys. Scr. 18, 499 (1978).

[21]K. Codling, J. Chem. Phys. 44, 4401 (1966).

[22]M. Nakamura, Y. Morioka, T. Hayaishi, E. Ishiguro, and M. Sasanuma, *Third International Conference on Vacuum Ultraviolet Radiation Physics* (Physical Society of Japan, Tokyo, 1971), paper 1pA1-6.

[23]L. C. Lee, E. Phillips, and D. L. Judge, J. Chem. Phys. 67, 1237 (1977).

[24]M. Sasanuma, E. Ishiguro, H. Masuko, Y. Morioka, and M. Nakamura, J. Phys. B 11, 3655 (1978).

[25]U. Gelius, J. Electron Spectrosc. Relat. Phenom. 5, 985 (1974).

[26]A. W. Potts, H. J. Lempka, D. G. Streets, and W. C. Price, Philos. Trans. R. Soc. London, Ser. A 268, 59

(1970).

[27]J. A. Sell and A. Kuppermann, Chem. Phys. 33, 379 (1978).

[28]T. Gustafsson, Phys. Rev. A 18, 1481 (1978).

[29]V. H. Dibeler and J. A. Walker, J. Chem. Phys. 44, 4405 (1966).

[30]M. Sasanuma, E. Ishiguro, T. Hayaisha, H. Masuko, Y. Morioka, T. Nakajima, and M. Nakamura, J. Phys. B 12, 4057 (1979).

[31]R. E. Kennerly, R. A. Bonham, and M. McMillan, J. Chem. Phys. 70, 2039 (1979).

[32]K. Rohr, J. Phys. B 12, L185 (1979).

[33]J. Simpson, C. Kuyatt, and S. Mielczarek, J. Chem. Phys. 44, 4403 (1966).

[34]S. Trajmar and A. Chutjian, J. Phys. B 10, 2943 (1977).

[35]A. P. Hitchcock and M. J. van der Wiel, J. Phys. B 12, 2153 (1979).

[36]A. Giardini-Guidoni, R. Fantoni, R. Tiribelli, D. Vinciguerra, R. Camilloni, and G. Stefani, J. Chem. Phys. 71, 3182 (1979).

[37]A. C. Parr, R. L. Stockbauer, B. E. Cole, D. L. Ederer, J. L. Dehmer, and J. B. West, Nucl. Instrum. Methods 172, 357 (1980).

[38]D. L. Ederer, B. E. Cole, and J. B. West, Nucl. Instrum. Methods 172, 185 (1980).

[30]G. V. Marr and J. B. West, At. Data Nucl. Data Tables 18, 497 (1976).

[40]J. L. Dehmer, W. A. Chupka, J. Berkowitz, and W. T. Jivery, Phys. Rev. A 12, 1966 (1975).

[41]J. Kreile and A. Schweig, J. Electron Spectrosc. Relat. Phenom. 20, 191 (1980).

[42]D. M. P. Holland, A. C. Parr, D. L. Ederer, J. L. Dehmer, and J. B. West, Nucl Instr. Methods 195, 331 (1982).

[43]J. A. R. Samson and A. F. Starace, J. Phys. B 8, 1806 (1975).

[44]J. L. Dehmer and D. Dill, in *Electron-Molecule and Photon-Molecule Collisions,* edited by T. Rescigno, V. McKoy, and B. Schneider (Plenum, New York, 1979), p. 225.

[45]J. R. Swanson, D. Dill, and J. L. Dehmer, J. Phys. B 13, L231 (1980); 14, L207 (1981).